
Manifestation of three-body forces in $f_{7/2}$ -shell nuclei.

ALEXANDER VOLYA

Department of Physics, Florida State University, Tallahassee, FL 32306-4350, USA

PACS 21.45.Ff – Three-nucleon forces

PACS 21.60.Cs – Shell model

PACS 21.30.-x – Nuclear forces

Abstract. – The traditional nuclear shell model approach is extended to include many-body forces. The empirical Hamiltonian with a three-body force is constructed for the identical nucleons on the $0f_{7/2}$ shell. Manifestations of the three-body force in spectra, binding energies, seniority mixing, particle-hole symmetry, electromagnetic and particle transition rates are investigated. It is shown that in addition to the usual expansion of the valence space within the traditional two-body shell model, the three-body component in the Hamiltonian can be an important part improving the quality of the theoretical approach.

The many-body problem is central for modern physics. A path from the understanding of interactions between fundamental constituents to that of the diverse physics of the whole system is non-trivial and involves various entangled routes. Among numerous issues, the questions of forces, effective or bare, their hierarchy and renormalizations are of particular importance. Nuclear physics is a valuable natural arena to explore this.

Microscopic treatments provide a remarkably accurate description of light nuclei based on the observed, bare, two-nucleon interactions [1]. The same calculations indicate that the role of three-body forces is increasingly large and non-perturbative for heavier systems. The many-body approaches with roots in effective interactions from mean-field (one-body) to shell model (one and two-body) indicate a need in empirical many-body force [2–4]. It is established that, regardless of ab-initio interactions, work in restricted space always gives rise to many-body forces; moreover, renormalizations may successfully set the hierarchy of importance [5, 6].

The goal of this work is to examine three-body forces within the nuclear shell model (SM) approach. This includes determination of effective interaction parameters, study of hierarchy in strength from single-particle (s.p.) to two-body to three-body and beyond, manifestations in energy spectra and transitions rates, comparison with different traditional SM calculations and overall assessment for the need of beyond-two-body SM. Previous works in this direction have shown improved description of energy spectra [2, 3, 7, 8] and the significance of three-body monopole renormalizations [4].

The effective interaction Hamiltonian is a sum $H_k = \sum_{n=1}^k H^{(n)}$ where the rotationally-invariant n -body part is

$$H^{(n)} = \sum_{\alpha\beta} \sum_L V_L^{(n)}(\alpha\beta) \sum_{M=-L}^L T_{LM}^{(n)\dagger}(\alpha) T_{LM}^{(n)}(\beta), \quad (1)$$

the isospin label is omitted here for the sake of simplicity. The operators $T_{LM}^{(n)\dagger}(\alpha)$ are normalized, i.e. $\langle 0 | T_{L'M'}^{(n)}(\alpha') T_{LM}^{(n)\dagger}(\alpha) | 0 \rangle = \delta_{\alpha\alpha'} \delta_{LL'} \delta_{MM'}$, n -body creation operators coupled to a total angular momentum L and magnetic projection M , $T_{LM}^{(n)\dagger}(\alpha) = \sum_{12\dots n} C_{12\dots n}^{LM}(\alpha) a_1^\dagger a_2^\dagger \dots a_n^\dagger$, where 1 is the s.p. index. The traditional SM approach is limited by the Hamiltonian $H_2 = H^{(1)} + H^{(2)}$ which is a sum of the s.p. ($n = 1$) and the two-body ($n = 2$) terms. In the two-body part the coefficients C_{12}^{LM} are proportional to the Clebsch-Gordan coefficients and the index α is uniquely identified by the s.p. levels involved. For $n > 2$ the index α must include additional information about the coupling scheme, the choice of which, in general, is not unique. In numerical work it is convenient to define the coefficients $C_{12\dots n}^{LM}(\alpha)$ and the normalized n -body operators $T_{LM}^{(n)}(\alpha)$ using a set of orthogonal eigenstates $|LM\alpha\rangle = T_{LM}^{(n)\dagger}(\alpha)|0\rangle$ of some n -particle system, see also [9].

Here we study identical nucleons in a single- j $0f_{7/2}$ shell; see Refs. [7, 10–13] for past works in this mass region. The best experimentally explored systems are $N = 28$ isotones starting from ^{48}Ca considered as a core with protons filling the $0f_{7/2}$ shell and the $Z=20$ $^{40-48}\text{Ca}$ isotopes with valence neutrons. The experimentally known states identified with the $f_{7/2}$ valence space are listed in Tab. 1.

The three-body interactions influence nuclear masses and result in important monopole terms [4]. The violation of particle-hole symmetry is related to this. Within the traditional SM in single j -shell, with occupancy $\Omega = 2j + 1$, this symmetry makes the spectra of the N and \tilde{N} -particle systems ($\tilde{N} = \Omega - N$) identical, apart from a constant shift in energy. Indeed, the particle-hole conjugation \mathcal{C} defined with $\tilde{a}_{jm}^\dagger \equiv \mathcal{C} a_{jm}^\dagger \mathcal{C}^{-1} = (-1)^{j-m} a_{j-m}$ transforms an arbitrary n -body interaction into itself plus some Hamiltonian of a lower interaction-rank H'_{n-1} , as follows: $\tilde{H}^{(n)} = (-1)^n H^{(n)} + H'_{n-1}$. The $n = 1$ case corresponds to the particle number $\tilde{N} = -N + \Omega$. For the $n = 2$ we obtain a monopole shift

$$\tilde{H}^{(2)} = H^{(2)} + (\Omega - 2N)M, \quad M = \frac{1}{\Omega} \sum (2L + 1)V_L^{(2)}. \quad (2)$$

Any $H^{(1)}$ is proportional to N and is thus a constant of motion, which explains the particle-hole symmetry for the two-body Hamiltonian. The $n \geq 3$ interactions violate this symmetry leading to different excitation spectra of N - and \tilde{N} -particle systems. The deviations from exact particle-hole symmetry are seen in the experimental data, Tab. 1. The excitation energies of $\nu = 2$ states in $N = 2$ system are systematically higher than those in the 6-particle case pointing on a reduced ground state binding.

The $j = 7/2$ is the largest single- j shell for which the seniority, the number ν of unpaired nucleons, is an integral of motion for any one- and two-body interaction [10, 14]. It is established experimentally that seniorities are mixed [15, 16]. Configurations beyond the single- j shell [8, 17–19] have been suggested to explain the effects; however, the possible presence of the three-body force must be addressed. In a single- j shell the pair operators $T_{00}^{(2)}$, $T_{00}^{(2)\dagger}$ and the particle number N form an SU(2) rotational quasispin group. The quantum numbers ν and N are associated with this group. The invariance under quasispin rotations relates states of the same ν but different particle numbers N . For example, excitation energies of $\nu = 2$ states are identical in all even-particle systems. The classification of operators according to quasispin leads to selection rules. The s.p. operators associated with the particle transfer permit seniority change $\Delta\nu = 1$. The reactions $^{51}\text{V}(^3\text{He}, \text{d})^{52}\text{Cr}$ and $^{43}\text{Ca}(\text{d}, \text{p})^{44}\text{Ca}$ show seniority mixing as the $\nu = 4$ final states are populated [16, 18]. The one-body multipole operators are quasispin scalars for odd angular momentum, and quasispin vectors for even. Thus, the $M1$ electromagnetic transitions do not change quasispin. In the mid-shell the quasi-vector $E2$ transitions between states of the same seniority are forbidden. The seniority mixing between the $\nu = 2$ and $\nu = 4$ pairs of 2^+ and 4^+ states is expected in the mid-shell nuclei ^{52}Cr and ^{44}Ca . Seniority can be used to classify the many-body operators $T_{LM}^{(n)}$ and the interaction parameters. The three-body interactions mix seniorities with the

		$N = 28$			$Z = 20$		
Spin	ν	Name	Binding	$3Bf_{7/2}$	Name	Binding	$3Bf_{7/2}$
0	0	^{48}Ca	0	0	^{40}Ca	0	0
7/2	1	^{49}Sc	9.626	9.753	^{41}Ca	8.360	8.4870
0	0	^{50}Ti	21.787	21.713	^{42}Ca	19.843	19.837
2	2	1.554	20.233	20.168	1.525	18.319	18.314
4	2	2.675	19.112	19.158	2.752	17.091	17.172
6	2	3.199	18.588	18.657	3.189	16.654	16.647
7/2	1	^{51}V	29.851	29.954	^{43}Ca	27.776	27.908
5/2	3	0.320	29.531	29.590	0.373	27.404	27.630
3/2	3	0.929	28.922	28.992	0.593	27.183	27.349
11/2	3	1.609	28.241	28.165	1.678	26.099	26.128
9/2	3	1.813	28.037	28.034	2.094	25.682	25.747
15/2	3	2.700	27.151	27.106	2.754	25.022	24.862
0	0	^{52}Cr	40.355	40.292	^{44}Ca	38.908	38.736
2 ₁	2 [*]	1.434	38.921	38.813	1.157	37.751	37.509
4 ₁	4 [*]	2.370	37.986	38.002	2.283	36.625	36.570
4 ₂	2 [*]	2.768	37.587	37.643	3.044	35.864	36.009
2 ₂	4 [*]	2.965	37.390	37.183	2.657	36.252	35.741
6	2	3.114	37.241	37.353	3.285	35.623	35.606
5	4	3.616	36.739	36.789	-	-	35.180
8	4	4.750	35.605	35.445	(5.088)	(33.821)	33.520
7/2	1	^{53}Mn	46.915	47.009	^{45}Ca	46.323	46.406
5/2	3	0.378	46.537	46.560	0.174	46.149	46.280
3/2	3	1.290	45.625	45.695	1.435	44.888	44.991
11/2	3	1.441	45.474	45.454	1.554	44.769	44.763
9/2	3	1.620	45.295	45.309	-	-	44.933
15/2	3	2.693	44.222	44.175	(2.878)	(43.445)	43.214
0	0	^{54}Fe	55.769	55.712	^{46}Ca	56.717	56.728,
2	2	1.408	54.360	54.286	1.346	55.371	55.501
4	2	2.538	53.230	53.307	2.575	54.142	54.332
6	2	2.949	52.819	52.890	2.974	53.743	53.659
7/2	2	^{55}Co	60.833	60.893	^{47}Ca	63.993	64.014
0	0	^{56}Ni	67.998	67.950	^{48}Ca	73.938	73.846

Table 1: States in $f_{7/2}$ valence space with spin and seniority listed in the first and second columns. A ^{*} denotes seniority mixed states in $3Bf_{7/2}$ and the seniority shown reflects the seniority assignment in the $2Bf_{7/2}$ model. In order to distinguish among the mixed states of the same spin-label (first column) we include an additional subscript reflecting the order in which they appear in the energy spectrum. Following are columns with data for $N = 28$ isotones and $Z = 20$ isotopes. Three columns for each type of valence particles list name and excitation energy, experimental binding energy, and energy from the three-body SM calculation discussed in the text. All energies are in MeV's.

exception of interaction between $\nu = 1$ nucleon triplets given by the strength $V_{7/2}^{(3)}$.

To determine the interaction parameters of H_3 we conduct a full least-square fit to the data points in Tab. 1. This empirical method, which dates back to Refs. [10, 20], is a part of the most successful SM techniques today [21]. Our procedure is similar to a two-body fit in sec. 3.2 of Ref. [22], but here the fit is nonlinear and requires iterations due to seniority mixing. In Tab. 2 the resulting parameters are listed for the proton (fixed $N = 28$) system

N=28		Z=20	
	2Bf _{7/2}	3Bf _{7/2}	2Bf _{7/2}
ϵ	-9827(16)	-9753(30)	-8542(35)
$V_0^{(2)}$	-2033(60)	-2207(97)	-2727(122)
$V_2^{(2)}$	-587(39)	-661(72)	-1347(87)
$V_4^{(2)}$	443(25)	348(50)	-164(49)
$V_6^{(2)}$	887(20)	849(38)	-198(130)
$V_{7/2}^{(3)}$		55(28)	53(70)
$V_{5/2}^{(3)}$		-18(70)	2(185)
$V_{3/2}^{(3)}$		-128(88)	-559(273)
$V_{11/2}^{(3)}$		102(43)	51(130)
$V_{9/2}^{(3)}$		122(41)	272(98)
$V_{15/2}^{(3)}$		-53(29)	-24(73)
RMS	120	80	220
			170

Table 2: Interaction parameters of 2Bf_{7/2} and 3Bf_{7/2} SM Hamiltonians determined with the least-square fit are given in keV's.

and neutron (fixed $Z = 20$) system. The two columns in each case correspond to fits without (2Bf_{7/2} left) and with (3Bf_{7/2} right) the three-body forces. The root-mean-square (RMS) deviation is given for each fit. The confidence limits can be inferred from variances for each fit parameter given within the parentheses.

The lowering of the RMS deviation is the first evidence in support of the three-body forces; for $Z = 28$ isotones it drops from 120keV to about 80keV. All three-body parameters appear to be equally important, excluding any one of them from the fit raises the RMS by about 10%. In contrast, inclusion of a four-body monopole force based on $\nu = 0$, $L = 0$ operator led to no improvement. The fit parameters remain stable within quoted error-bars if some questionable data-points are removed. The energies resulting from the three-body fit are listed in Tab. 1. Based on the RMS alone this description of data is quite good, even in comparison with the available large-scale two-body SM calculations in the expanded model space [19, 23].

The proton and neutron effective Hamiltonians are different, Tab. 2. The s.p. energies reflect different mean fields; and the two-body parameters, especially for higher L , highlight the contribution from the long range Coulomb force. However, within the error-bars the three-body part of the Hamiltonians appears to be the same which relates these terms to isospin-invariant strong force.

A skeptic may question some experimental states included in the fit, thus we conduct a minimal fit considering binding energies of ground states only, similar to Ref. [10]. We include a seniority conserving part given by $V_{7/2}^{(3)}$ with $\nu = 1$ triplet operator $T_{jm}^{(3)} \sim a_{jm}^\dagger T_{00}^{(2)}$. This interaction is the main three-body contribution to binding and is equivalent to a density-dependent pairing force [24]. In a single- j model it can be treated exactly with a renormalized particle-number-dependent pairing strength $V_0^{(2)'} = V_0^{(2)} + \Omega \frac{N-2}{\Omega-2} V_j^{(3)}$. From relations in Refs. [10, 13], the ground state energies with $\nu = 0$ or 1 are

$$E = \epsilon N + \frac{N - \nu}{\Omega - 2} \left((\Omega - N - \nu) \frac{V_0^{(2)'}}{2} + (N - 2 + \nu) M' \right), \quad (3)$$

where $M' = M + \frac{N-2}{\Omega-2} V_j^{(3)}$. With a linear least-square fit and Eq. (3) we determine s.p.

	$N = 28$		$Z = 20$	
ϵ	-9703(40)	-9692(40)	-8423(51)	-8403(55)
$V_0^{(2)}$	-2354(80)	-2409(110)	-3006(120)	-3105(156)
M	1196(40)	1166(50)	-823(55)	-876(76)
$V_{7/2}^{(3)}$	-	18(20)	-	31(31)
RMS	50	46	73	65

Table 3: Interaction parameters for the minimal $f_{7/2}$ SM determined with the linear least-squared fit of 8 binding energies. The variances for each parameter are shown within parentheses. The two columns for isotopes and isotones are fits without and with the three-body term.

energy ϵ , pairing $V_0^{(2)}$, monopole M , and 3-body interaction $V_{7/2}^{(3)}$ (3) using 8 binding energies. The results, shown in Tab 3, are consistent with the full fit in Tab. 2, the repulsive nature of the monopole $V_{7/2}^{(3)}$ is in agreement with other works [25].

Next we concentrate on ^{52}Cr , Fig. 1. In addition to the $2\text{B}f_{7/2}$ and $3\text{B}f_{7/2}$ interactions from Tab. 2 we perform a large-scale SM calculations $2\text{B}f_{7/2}p$ (which includes $p_{1/2}$ and $p_{3/2}$) and $2\text{B}fp$ (entire fp -shell, truncated to 10^7 projected m-scheme states) using FPPB two-body SM Hamiltonian [26]. The $2\text{B}f_{7/2}p$ model and its results are very close to the more restricted SM calculations in Ref. [23].

The seniority mixing between the neighboring 4_1^+ and 4_2^+ states leads to level repulsion. The observed energy difference of 400 keV is not reproduced by $2\text{B}f_{7/2}$ (84 keV). The discrepancy remains in some of the extended two-body models: $2\text{B}f_{7/2}p$ and [23] (200 keV). The full $2\text{B}fp$ replicates the splitting, but possibly at the expense of excessive intruder admixtures which distort the spectrum, see also Ref. [27]. The $3\text{B}f_{7/2}$ is the best in reproducing the experimental spectrum, Fig. 1. The $3\text{B}f_{7/2}$ model predicts seniority mixing; the $\nu(4_1^+) = 2.82$ and $\nu(4_2^+) = 2.71$ are inferred from the expectation value of the pair operator $\langle T_{00}^{(2)\dagger} T_{00}^{(2)} \rangle = (N - \nu)(2j + 3 - N - \nu)/(4j + 2)$. The 2_1^+ , however, is relatively pure with $\nu(2_1^+) = 2.006$.

Violations of the quasispin selection rules are observed in nuclei [12, 15, 16, 28, 29]. The

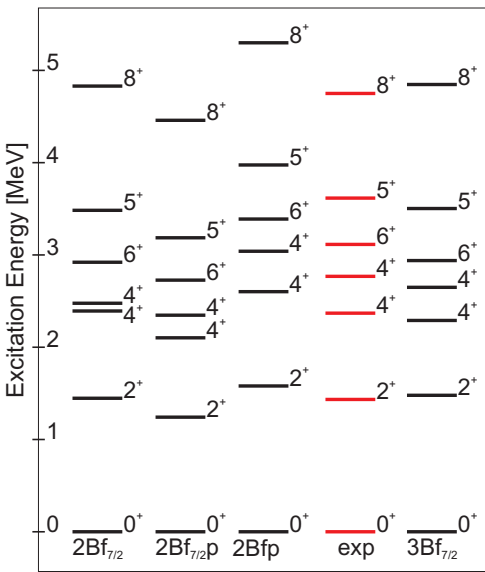


Fig. 1: Spectrum of ^{52}Cr .

	$2Bf_{7/2}$	$2Bf_{7/2}p$	$2Bfp$	$3Bf_{7/2}$	Experiment
$2_1 \rightarrow 0^{(*)}$	118.0	118.0	118	117.5	118 ± 35
$4_1 \rightarrow 2_1$	130.4	122.5	105.8	73.2	$83 \pm 15^{(1,2)}$
$4_2 \rightarrow 2_1$	0	3.3	15.1	56.8	69 ± 18
$4_2 \rightarrow 4_1$	125.2	59.3	2.6	0.5	
$2_2 \rightarrow 0$	0	0.003	0.9	0.5	0.06 ± 0.05
$2_2 \rightarrow 2_1$	119.2	102.2	101.9	117.1	150 ± 35
$2_2 \rightarrow 4_1$	0	10.8	34.4	19.9	
$2_2 \rightarrow 4_2$	57.8	7.2	5.2	38.7	
$6 \rightarrow 4_1$	108.9	86.2	56.3	57.8	$59 \pm 20^{(1)}$
$6 \rightarrow 4_2$	0	9.3	27.6	51.1	$30 \pm 10^{(1)}$
$Q(2_1^+)$ $e\text{ fm}^2$	0	-13.0	-13.4 ⁽³⁾	-2.4	$-8.2 \pm 1.6^{(4)}$

Table 4: $B(E2)$ transition summary on ^{52}Cr expressed in units $e^2 \text{ fm}^4$, the last row being the quadrupole moment of the first 2^+ state in units $e \text{ fm}^2$. The data is taken from [31]. The zeros in the second column for the $2Bf_{7/2}$ model are the results of the mid-shell seniority selection rules. In this model the states 2_1 , 2_2 , 4_1 , and 4_2 have seniorities 2, 4, 4, and 2, respectively, see Tab. 1. ^(*)In $2Bf_{7/2}p$ and $2Bfp$ models we use 0.5 (neutron) and 1.5 (proton) effective charges. The overall radial scaling is fixed by $B(E2, 2_1 \rightarrow 0)$. ⁽¹⁾The life-time error-bars are used. ⁽²⁾There are conflicting experimental results on the life-time; here we use DSAM (HI, $xn\gamma$) data from Ref. [31], which is consistent with [30]. ⁽³⁾Other independent large-scale shell model calculations obtain similar values for the quadrupole moment for the 2_1^+ state: -12.3 [32], -15.0, -16.2 and -17.5 [33], all in units $e \text{ fm}^2$. ⁽⁴⁾ The experimental data is from [34].

two-body shell models beyond single- j $f_{7/2}$ are used to explain this seniority mixing [11, 12, 17, 18, 23], however there are inconsistencies, suggesting a more in-depth consideration. Large variations of effective charges are needed to explain electromagnetic transitions [30]. The particle transfer spectroscopic factors show excessive amount of components outside the $f_{7/2}$ valence space [15]. Furthermore, while going beyond the single j -shell is imperative to account for the observed g factors [22], the agreement between the experiment and the common large-scale shell model results is not perfect, Ref. [27], which may be a hint for the presence of a three-body force.

In Tab. 4 $B(E2)$ transitions rates from the four models are compared to experiment. The combination of nuclear radial overlap and effective charge is normalized using the observed $E2$ rate for the transition $2_1 \rightarrow 0$ in the $2Bf_{7/2}$, $2Bf_{7/2}p$, and $2Bfp$ models. The normalization parameter for the $3Bf_{7/2}$ model is identical to the one used in $2Bf_{7/2}$. The insignificant difference in $2_1 \rightarrow 0$ $B(E2)$ between the $3Bf_{7/2}$ and $2Bf_{7/2}$ shows a small admixture of $\nu = 4$ in the 2_1^+ state. The $\nu = 4$ and $\nu = 2$ mixing in 4_1^+ and 4_2^+ effects the transitions involving these states. For example, $E2$ transitions $4_2 \rightarrow 2_1$ and $6 \rightarrow 4_2$ are no longer forbidden.

The last row in Tab. 4 compares the quadrupole moment of the first 2^+ state in ^{52}Cr between models and experiment. It is quoted in units of $e \text{ fm}^2$. Because of the seniority selection rule the quadrupole moment is exactly zero in the $2Bf_{7/2}$ model; the small seniority mixing between 2^+ states in the $3Bf_{7/2}$ model leads to the quadrupole moment of a correct sign but it is lower than the observed one. The results from extended two-body models in Tab. 4 and in the literature [32, 33, 35] improve the picture. However, strong configuration mixing is needed to generate seniority mixing which is inconsistent with g factor measurements [27] and results in a quadrupole moment higher than observed. This again invites the possibility of an additional three-body Hamiltonian.

In Tab. 5 proton removal spectroscopic factors are compared between theoretical models and experiment $^{51}\text{V}(\text{He}, \text{d})^{52}\text{Cr}$ [15]. The $3Bf_{7/2}$ model is good in its description of observation especially for the 4_1^+ and 4_2^+ states. It was pointed out in Ref. [15] that the

	2Bf _{7/2}	2Bf _{7/2} p	2Bfp	3Bf _{7/2}	Exp
0 ⁺	4.00	3.73	3.40	4.00	4.00
2 ₁ ⁺	1.33	1.14	0.94	1.33	1.08
4 ₁ ⁺	0.00	0.13	0.34	0.63	0.51
4 ₂ ⁺	1.33	1.11	0.70	0.71	0.81
6 ⁺	1.33	1.28	1.28	1.33	1.31

Table 5: Proton removal spectroscopic factors. The experimental data is taken from $^{51}\text{V}(^{3}\text{He},\text{d})^{52}\text{Cr}$ reaction [15]. Within error-bars of about 0.1 this data is consistent with other results [31].

spectroscopic factors for the 4⁺ states probe the $\nu = 2$ component, and, thus, their sum within the $f_{7/2}$ valence space is 4/3; this result is consistent with the observation [15] but does not support too much configuration mixing from outside the $f_{7/2}$ shell which would reduce the spectroscopic factors and their sum.

To conclude, the study of nuclei in 0f_{7/2} shell shows evidence for three-body forces. We extend the traditional shell model approach by including three-body forces into consideration, we find that a successful set of interaction parameters can be determined with an empirical fitting procedure. With a few new parameters a sizable improvement in the description of experimental data is obtained. The apparent hierarchy of contributions from one-body mean-field, to two-body, to three-body and beyond is significant; it assures the possibility of high precision configuration-interaction methods in restricted space and supports ideas about renormalization of interactions. The three-body forces observed in this study appear to be isospin invariant. The new Hamiltonian with three-body forces describes well the observables that are sensitive to such forces and to seniority, and particle-hole symmetries that are violated in their presence. A good experimental agreement is obtained for the features of spectra, for electromagnetic E2 transition rates, and for spectroscopic factors. While good agreement with experiment can also be obtained by configuration mixing within some advanced large-scale two-body shell model calculations, it appears that the three-body effective interaction has a somewhat different manifestation which can be experimentally identified. In particular, with the three-body force, the seniority forbidden transitions become allowed without generating excessively large quadrupole moment or, in the case of spectroscopic factors, without loosing too much strength away from a single- j shell. Unlike the fit to experimental data discussed in this work, it appears to be difficult to fit the large-scale shell model results with a single- j Hamiltonian containing a three-body force. This again suggests that configuration mixing is not necessarily equivalent to a three-body force. The work in this direction is to be continued. It is important to conduct similar phenomenological investigations for other mass regions and model spaces; on the other side, renormalization techniques that would link fundamental and phenomenological forces [5] have to be searched for.

The author is thankful to N. Auerbach and V. Zelevinsky for enlightening discussions. Support from the U. S. Department of Energy, grant DE-FG02-92ER40750 is acknowledged.

REFERENCES

- [1] PIEPER S. C., PANDHARIPANDE V. R., WIRINGA R. B. and CARLSON J., *Phys. Rev. C*, **64** (2001) 014001.
- [2] VAN HEES A., BOOTEN J. and GLAUDEMANS P., *Phys. Rev. Lett.*, **62** (1989) 2245.
- [3] VAN HEES A., BOOTEN J. and GLAUDEMANS P., *Nucl. Phys.*, **A507** (1990) 55.
- [4] ZUKER A. P., *Phys. Rev. Lett.*, **90** (2003) 042502.

- [5] SCHWENK A. and HOLT J. D., arXiv:0802.3741 (2008).
- [6] BARRETT B., DEAN D., HJORTH-JENSEN M., and VARY J., *J. Phys. G*, **31** (2005) .
- [7] EISENSTEIN I. and KIRSON M. W., *Phys. Lett.*, **B47** (1973) 315.
- [8] POVES A. and ZUKER A., *Phys. Rep.*, **70** (1981) 235.
- [9] VOLYA A., *Phys. Rev. Lett.*, **100** (2008) 162501.
- [10] TALMI I., *Phys. Rev.*, **107** (1957) 326.
- [11] GINOCCHIO J. N. and FRENCH J. B., *Phys. Lett.*, **7** (1963) 137.
- [12] MCCULLEN J. D., BAYMAN B. F. and ZAMICK L., *Phys. Rev.*, **134** (1964) B515.
- [13] VOLYA A., *Phys. Rev. C*, **65** (2002) 044311.
- [14] SCHWARTZ C. and DESHALIT A., *Phys. Rev.*, **94** (1954) 1257.
- [15] ARMSTRONG D. D. and BLAIR A. G., *Phys. Rev.*, **140** (1965) B1226.
- [16] BJERREGAARD J. H. and HANSEN O., *Phys. Rev.*, **155** (1967) 1229.
- [17] ENGELAND T. and OSNES E., *Phys. Lett.*, **20** (1966) 424.
- [18] AUERBACH N., *Phys. Lett.*, **B24** (1967) 260.
- [19] POVES A., SANCHEZ-SOLANO J., CAURIER E. and NOWACKI F., *Nucl. Phys.*, **A694** (2001) 157.
- [20] BACHER R. F. and GOUDSMIT S., *Phys. Rev.*, **46** (1934) 948.
- [21] BROWN B. A. and RICHTER W. A., *Phys. Rev. C*, **74** (2006) 034315.
- [22] LAWSON R. D., *Theory of the nuclear shell model* (Clarendon Press) 1980.
- [23] LIPS K. and MCCELLISTREM M. T., *Phys. Rev. C*, **1** (1970) 1009.
- [24] ZELEVINSKY V., SUMARYADA T. and VOLYA A., <http://meeting.aps.org/link/BAPS.2006.APR.C8.4> (2006).
- [25] COON S. A., PENA M. T. and RISKA D. O., *Phys. Rev. C*, **52** (1995) 2925.
- [26] BROWN B. A., *Prog. Part. Nucl. Phys.*, **47** (2001) 517.
- [27] SPEIDEL K.-H. and *et al.*, *Phys. Rev. C*, **62** (2000) 031301(R).
- [28] MONAHAN C. F. and *et al.*, *Nucl. Phys.*, **A120** (1968) 460.
- [29] PELLEGRINI F., FILOSOFO I., ZAIKI M. I. E. and GABRIELLI I., *Phys. Rev. C*, **8** (1973) 1547.
- [30] BROWN B. A., FOSSAN D. B., McDONALD J. M. and SNOVER K. A., *Phys. Rev. C*, **9** (1974) 1033.
- [31] HUO J., HUO S. and MA C., *Nuclear Data Sheets*, **108** (2007) 773.
- [32] HONMA M., OTSUKA T., BROWN B. A. and MIZUSAKI T., *Phys. Rev. C*, **69** (2004) 034335.
- [33] MUKHERJEE G. and SHARMA S.K., *Phys. Rev. C*, **29** (1984) 2101.
- [34] RAGHAVAN P., *At. Data Nucl. Data. Tab.*, **42** (1989) 189.
- [35] ERNST R. and *et al.*, *Phys. Rev. Lett.*, **84** (2000) 416.